Available online at www.sciencedirect.com
SCIENCE DIRECT®
Engineering Fracture Mechanics 72 (2005) 2128–2143
Engineering Fracture Mechanics
www.elsevier.com/locate/engfracmech

A new boundary integral equation method for cracked 2-D anisotropic bodies

Yin-Bang Wang [a], Yu-Zhou Sun [b,*]

[a] Engineering College, Ocean University of China, Qingdao 260071, China
[b] Department of Basic Science, Zhongyuan Institute of Technology, 41 Zhongyuan West Road, Zhengzhou, Henan 450007, China

Received 25 January 2001; received in revised form 14 January 2005; accepted 25 January 2005
Available online 27 April 2005

Abstract

By using integration by parts to the traditional boundary integral formulation, a traction boundary integral equation for cracked 2-D anisotropic bodies is derived. The new traction integral equation involves only singularity of order $1/r$ and no hypersingular term appears. The dislocation densities on the crack surface are introduced and the relations between stress intensity factors and dislocation densities near the crack tip are induced to calculate the stress intensity factors. The boundary element method based on the new equation is established and the singular interpolation functions are introduced to model the singularity of the dislocation density (in the order of $1/\sqrt{r}$) for crack tip elements. The proposed method can be directly used for the 2-D anisotropic body containing cracks of arbitrary geometric shapes. Several numerical examples demonstrate the validity and accuracy of BEM based on the new boundary integral equation.

Keywords: Anisotropic; Cracks; Dislocation densities; Boundary integral equation; Stress intensity factors

1. Introduction

Boundary element method has been proved to be a powerful tool for solving fracture mechanics problems, but the traditional displacement BEM cannot be directly applied to crack problems because of the geometrical overlapping of the upper and lower crack surfaces. Previously, many approaches within the scope of the BEM have been devised to overcome this difficulty. The first one is the Green's function method [1], and the other approaches, such as the subregional method [2,3]; the displacement discontinuity

* Corresponding author. Tel.: +86 371 8952576; fax: +86 371 7978062.
E-mail address: yuzhousun@yahoo.com.cn (Y.-Z. Sun).

0013-7944/$ - see front matter © 2005 Elsevier Ltd. All rights reserved.
doi:10.1016/j.engfracmech.2005.01.007

method (DDM) [4]; the dual or hypersingular boundary element method [5–7], have also been successfully applied in many cases. A newly developed skill is the dislocation density method [8–11], and this technique reduces the singularity by one order using integration by parts and expressing the unknowns as dislocation densities on the crack surface. Wang [10,11] used integration by parts to 2-D and 3-D displacement boundary integral formulation to derive the traction integral equations, and analyzed the Griffith crack problems and 3-D crack problems. Noticing some particular relations, Chau and Wang [12,13] obtained a more universal boundary integral formulation for 2-D bodies containing holes and cracks, and represented them in the complex variable notation. In addition, Richardson and Cruse [14] directly applied integration by parts to the traction integral formulations and gave a weakly singular stress-BEM for 2-D isotropic crack problem. Li et al. [15] applied integration by parts to the 3-D isotropic crack problems, and the hypersingular integral is bypassed in their equation, but the displacement and traction boundary integral equations are required for the general boundary and crack surface (i.e. it is a dual BEM method). Compared with the methods of Richardson and Cruse [14] and Li et al. [15], the boundary integral equations of Wang [11] and Chau and Wang [12] seem to be more complete and regular.

The general fracture mechanics problems of anisotropic media have been studied by many investigators [3,16–19] with the boundary collocation method, the finite element method or other techniques. In the area of BEM for cracked 2-D anisotropic media, to our knowledge, Snyder and Cruse [1] firstly obtained the Green's functions for the infinite anisotropic plate with a straight crack and incorporated them in the boundary element analysis; Kamel and Liaw [20] derived the Green's functions for the infinite anisotropic plate containing an elliptical hole and used them as the kernels of the integral formulation; Doblare et al. [21] and Sollero and Aliabadi [2] used the traditional displacement boundary integral equation to analyze cracked bodies with geometric symmetry; Pan and Amadei [22] proposed a new BEM formulation on the basis of dual boundary element method and the displacement discontinuity DDM, and Gray and Paulino [23] presented a symmetric Galerkin boundary integral method for two dimensional linear elastic orthotropic fracture analysis, but their traction equations [22,23] involve singularity of order $1/r^2$ and the treatments of hypersingular integrals are complex. In this paper, we extend the method and techniques of Chau and Wang [12] to the cracked 2-D anisotropic media, and a new traction boundary integral equation is obtained.

In our method, the traction sum $\sum t_i$ of the upper and lower, generally equal to zero, is not directly omitted from the displacement boundary integral formulation. Integration by parts is used and the tangential derivative of the displacement is introduced. Our traction integral equation is regular and complete for 2-D anisotropic crack problems, and in the application, no displacement integral equation is required (not like the dual BEM). The integral kernels only involve the singularity of order $1/r$, and this characteristic leads to the analytical evaluation of all singular integral. Another merit is that the application to the curved crack is very convenient because the derivative of dislocation is about the tangential direction of the crack surface.

The boundary element method based on the traction integral equation is established. The linear interpolation is used for general elements, and singular interpolation functions are introduced for the crack tip elements to model the singularity of the dislocation densities. The stress intensity factors can be calculated from the dislocation densities. Numerical examples with straight or curved cracks show the proposed method is simple, accurate and easily applicable to cracked 2-D anisotropic media.

2. Fundamental solutions for the 2-D anisotropic media

2.1. Basic formulations

Under the assumption that the anisotropic of the material is symmetric about the plane (x_1, x_2), i.e. the third material principle axis is perpendicular to the plane (x_1, x_2), the governing equations for the plane stress problem of anisotropic media are [24]:

$$\sigma_{ij,j} = 0, \tag{1}$$

$$\varepsilon_{ik} = \frac{1}{2}(u_{i,k} + u_{k,i}), \tag{2}$$

$$\begin{Bmatrix} \varepsilon_{11} \\ \varepsilon_{22} \\ 2\varepsilon_{12} \end{Bmatrix} = \begin{bmatrix} s_{11} & s_{12} & s_{16} \\ s_{12} & s_{22} & s_{26} \\ s_{16} & s_{26} & s_{66} \end{bmatrix} \begin{Bmatrix} \sigma_{11} \\ \sigma_{22} \\ \sigma_{12} \end{Bmatrix}, \tag{3}$$

where s_{ij} are the elements of the compliance matrix.

For the plane strain problem, Eq. (3) should be replaced by

$$\begin{Bmatrix} \varepsilon_{11} \\ \varepsilon_{22} \\ 2\varepsilon_{12} \end{Bmatrix} = \begin{bmatrix} \beta_{11} & \beta_{12} & \beta_{16} \\ \beta_{12} & \beta_{22} & \beta_{26} \\ \beta_{16} & \beta_{26} & \beta_{66} \end{bmatrix} \begin{Bmatrix} \sigma_{11} \\ \sigma_{22} \\ \sigma_{12} \end{Bmatrix}, \tag{4}$$

where $\beta_{ij} = s_{ij} - s_{i3}s_{j3}/s_{33}$ $(i,j = 1,2,6)$.

The inverse of Eqs. (3) and (4) can be expressed as

$$\begin{Bmatrix} \sigma_{11} \\ \sigma_{22} \\ \sigma_{12} \end{Bmatrix} = \begin{bmatrix} d_{11} & d_{12} & d_{16} \\ d_{12} & d_{22} & d_{26} \\ d_{16} & d_{26} & d_{66} \end{bmatrix} \begin{Bmatrix} \varepsilon_{11} \\ \varepsilon_{22} \\ 2\varepsilon_{12} \end{Bmatrix}, \tag{5}$$

where $[d_{qr}]$ is the inverse of matrix $[s_{qr}]$ or $[\beta_{qr}]$.

The stress–displacement relationship can also be written in a tensor form as [22,24]

$$\sigma_{lm} = c_{lmij}\varepsilon_{ij} = c_{lmij}\frac{\partial u_i}{\partial x_j}, \tag{6}$$

in which c_{lmij} are the components of the stiffness tensor of the anisotropic medium, and for the plane problem the magnitudes of the components $c_{lmij}(l,i,j,m = 1,2)$ are easily obtained from d_{qr} [24].

2.2. Fundamental solutions

Firstly, we introduce complex variables

$$z_1 = x_1 + \mu_1 x_2, \quad z_2 = x_1 + \mu_2 x_2, \tag{7}$$

where the complex variables μ_1, μ_2 are the two roots of the characteristic equation

$$a_{11}\mu^4 - 2a_{16}\mu^3 + (2a_{12} + a_{66})\mu^2 - 2a_{26}\mu + a_{22} = 0, \tag{8}$$

with $a_{ij} = s_{ij}$ for plane stress problems and $a_{ij} = \beta_{ij}$ for plane strain problems.

The roots of Eq. (8) are either complex or purely imaginary and cannot be real [25]. In what follows, μ_1, $\bar{\mu}_1$, μ_2 and $\bar{\mu}_2$ denote the four roots with the overbar designating complex conjugates.

The fundamental solutions and $U_{kl}(z_0,z)$ and $T_{kl}(z_0,z)$ are the lth displacement and traction at field point $z(x_1,x_2)$ caused by a unit point force along the kth direction at a source point $z_0(x_{01},x_{02})$.

Displacement fundamental solutions $U_{kl}(z_0,z)$ can be expressed as following [2,22,26]:

$$U_{kl}(z_0,z) = 2Re[P_{l1}A_{k1}\ln(z_1 - z_{01}) + P_{l2}A_{k2}\ln(z_2 - z_{02})]. \tag{9}$$

For the convenience of the further application, we can write traction fundamental solution $T_{kl}(z_0,z)$ in the form

$$T_{kl}(z_0,z) = -D_{klj}(z_0,z)\cdot n_j(z) \tag{10}$$

with

$$D_{k2i}(z_0,z)=2Re\left[\sum_{j=1}^{2}L_{ij}A_{kj}\frac{1}{z_j-z_{0j}}\right],$$
$$D_{k1i}(z_0,z)=-2Re\left[\sum_{j=1}^{2}L_{ij}\mu_jA_{kj}\frac{1}{z_j-z_{0j}}\right], \tag{11}$$

in which $n_j(z)$ are the outward normal components of the field point $z(x_1,x_2)$ and

$$[L_{ij}]=\begin{bmatrix}\mu_1 & \mu_2\\ -1 & -1\end{bmatrix}, \tag{12}$$

$$[P_{ik}]=\begin{bmatrix}a_{11}\mu_k^2+a_{12}-a_{16}\mu_k\\ a_{12}\mu_k+a_{22}/\mu_k-a_{26}\end{bmatrix}. \tag{13}$$

Complex variables A_{ij} can be obtained from the solutions of the linear system

$$\begin{bmatrix}1 & -1 & 1 & -1\\ \mu_1 & -\overline{\mu}_1 & \mu_2 & -\overline{\mu}_2\\ P_{11} & -\overline{P}_{11} & P_{12} & -\overline{P}_{12}\\ P_{21} & -\overline{P}_{21} & P_{22} & -\overline{P}_{22}\end{bmatrix}\begin{Bmatrix}A_{j1}\\ \overline{A}_{j1}\\ A_{j2}\\ \overline{A}_{j2}\end{Bmatrix}=\frac{1}{2\pi i}\begin{Bmatrix}\delta_{j2}\\ -\delta_{j1}\\ 0\\ 0\end{Bmatrix}. \tag{14}$$

3. The new boundary integral equation

From the fundamental solutions $U_{kl}(z_0,z)$ and $T_{kl}(z_0,z)$, the traditional displacement boundary integral formulation can be expressed as [27]

$$u_i(z_0)=\int_S U_{ij}(z_0,z)t_j(z)\mathrm{d}s(z)-\int_S T_{ij}(z_0,z)u_j(z)\mathrm{d}s(z)+\int_\Gamma U_{ij}(z_0,z)\sum t_j(z)\mathrm{d}s(z)$$
$$-\int_\Gamma T_{ij}(z_0,z)\Delta u_j(z)\mathrm{d}s(z), \tag{15}$$

where $s(z)$ is the arc length along the boundary S or crack surface Γ and $i,j=1,2$; $\Delta u_j(z)=u_j^+(z)-u_j^-(z)$ is the difference of the displacements between the upper and lower crack surfaces; $\sum t_j(z)=t_j^+(z)+t_j^-(z)$ is the sum of the tractions acting on the upper and lower crack surfaces. Generally, $\sum t_j$ is equal to zero, but it is not directly omitted at present, and this will lead to a different equation in comparison to the general traction boundary integral equation.

Since the displacement field given in (15) is valid at all internal points of linear elastic body, thus Hook's law can be applied to obtain the stress field inside the body. In particular, we first differentiate $u_i(z_0)$ with respect to x_{0k} to give

$$\frac{\partial u_i(z_0)}{\partial x_{0k}}=\int_S\frac{\partial U_{ij}(z_0,z)}{\partial x_{0k}}t_j(z)\mathrm{d}s(z)-\int_S\frac{\partial T_{ij}(z_0,z)}{\partial x_{0k}}u_j(z)\mathrm{d}s(z)+\int_\Gamma\frac{\partial U_{ij}(z_0,z)}{\partial x_{0k}}\sum t_j(z)\mathrm{d}s(z)$$
$$-\int_\Gamma\frac{\partial T_{ij}(z_0,z)}{\partial x_{0k}}\Delta u_j(z)\mathrm{d}s(z). \tag{16}$$

From the fact that $\partial(z_j - z_{0j})/\partial x_{0k} = -\partial(z_j - z_{0j})/\partial x_k$, it can be seen that

$$\frac{\partial U_{ij}(z_0,z)}{\partial x_{0k}} = -\frac{\partial U_{ij}(z_0,z)}{\partial x_k} = -U_{ij,k}(z_0,z). \tag{17}$$

Obviously, the fundamental solutions $D_{ijk}(z_0,z)$ should also satisfy the equilibrium equation (1), therefore we have

$$\frac{\partial D_{ij1}(z_0,z)}{\partial x_1} = -\frac{\partial D_{ij2}(z_0,z)}{\partial x_2}, \quad \text{for } z \neq z_0. \tag{18}$$

Noting the relation that $\partial D_{ijk}(z_0,z)/\partial x_{0l} = -\partial D_{ijk}(z_0,z)/\partial x_l$ and Eq. (18), we can differentiate $T_{ij}(z_0,z)$ given in (10) with respect to x_{01} to give

$$\begin{aligned}\frac{\partial T_{ij}(z_0,z)}{\partial x_{01}} &= -\left(n_1\frac{\partial D_{ij1}(z_0,z)}{\partial x_{01}} + n_2\frac{\partial D_{ij2}(z_0,z)}{\partial x_{01}}\right) = n_1\frac{\partial D_{ij1}(z_0,z)}{\partial x_1} + n_2\frac{\partial D_{ij2}(z_0,z)}{\partial x_1} \\ &= -\left(-n_2\frac{\partial}{\partial x_1} + n_1\frac{\partial}{\partial x_2}\right)D_{ij2}(z_0,z) = -\frac{\partial D_{ij2}(z_0,z)}{\partial s(z)},\end{aligned} \tag{19}$$

the last of (19) is resulted from the following identity:

$$\partial f/\partial s = n_1(\partial f/\partial x_2) - n_2(\partial f/\partial x_1).$$

Similar procedure gives

$$\frac{\partial T_{ij}(z_0,z)}{\partial x_{02}} = \frac{\partial D_{ij1}(z_0,z)}{\partial s(z)}. \tag{20}$$

Eqs. (19) and (20) can be written in a more compact form as

$$\frac{\partial T_{ij}(z_0,z)}{\partial x_{0k}} = -e_{k\beta}\frac{\partial D_{ij\beta}(z_0,z)}{\partial s(z)}, \tag{21}$$

where $e_{ij} = \delta_{1i}\delta_{2j} - \delta_{2i}\delta_{1j}$ is 2-D permutation tensor (i.e. $e_{11} = e_{22} = 0$, $e_{12} = -e_{21} = 1$).

Substituting Eqs. (17) and (21) into (16) and inserting the expression for $\partial u_i(z_0)/\partial x_{0k}$ into Eq. (6) yield

$$\begin{aligned}\sigma_{lm}(z_0) = &-\int_S c_{lmik}U_{ij,k}(z_0,z)t_j(z)\mathrm{d}s(z) + \int_S \frac{\partial W_{jlm}(z_0,z)}{\partial s(z)}u_j(z)\mathrm{d}s(z) - \int_\Gamma c_{lmik}U_{ij,k}(z_0,z)\sum t_j(z)\mathrm{d}s(z) \\ &+ \int_\Gamma \frac{\partial W_{jlm}(z_0,z)}{\partial s(z)}\Delta u_j(z)\mathrm{d}s(z),\end{aligned} \tag{22}$$

where $W_{jlm}(z_0,z) = c_{lmik}e_{k\beta}D_{ij\beta}(z_0,z)$.

Integrating (22) by parts and noting that $[W_{jlm}u_j]$ vanishes around a closed boundary S since it is a single-value function and $[W_{jlm}\Delta u_j]$ vanishes on both tips of any crack Γ, thus we obtain

$$\begin{aligned}\sigma_{lm}(z_0) = &-\int_S c_{lmik}U_{ij,k}(z_0,z)t_j(z)\mathrm{d}s(z) - \int_S W_{jlm}(z_0,z)\frac{\partial u_j(z)}{\partial s(z)}\mathrm{d}s(z) \\ &- \int_\Gamma c_{lmik}U_{ij,k}(z_0,z)\sum t_j(z)\mathrm{d}s(z) - \int_\Gamma W_{jlm}(z_0,z)\frac{\partial \Delta u_j(z)}{\partial s(z)}\mathrm{d}s(z).\end{aligned} \tag{23}$$

Assuming that the point z_0' is a point on the smooth boundary S or crack surface Γ and $n_1(z_0')$, $n_2(z_0')$ are the outward normal components of the point z_0', the traction at the point z_0' can be expressed as

$$t_l(z_0') = \lim_{z_0 \to z_0'}[\sigma_{lm}(z_0)n_m(z_0')]. \tag{24}$$

After substituting (23) into (24) and doing a limiting operation, we finally obtain (z_0' is rewritten as z_0)

$$\begin{aligned}
&-n_m(z_0)\int_S c_{lmik}U_{ij,k}(z_0,z)t_j(z)\mathrm{d}s(z) - n_m(z_0)\int_S W_{jlm}(z_0,z)\frac{\partial u_j(z)}{\partial s(z)}\mathrm{d}s(z)\\
&-n_m(z_0)\int_\Gamma c_{lmik}U_{ij,k}(z_0,z)\sum t_j(z)\mathrm{d}s(z) - n_m(z_0)\int_\Gamma W_{jlm}(z_0,z)\frac{\partial \Delta u_j(z)}{\partial s(z)}\mathrm{d}s(z)\\
&=\begin{cases}\frac{1}{2}t_l(z_0) & z_0\in s\\ \frac{1}{2}(t_l(z_0^+)-t_l(z_0^-)) & z_0\in \Gamma\end{cases},
\end{aligned} \tag{25}$$

in which $t_l(z_0^+)-t_l(z_0^-)$ is the difference of the tractions between the upper and lower crack surface. Of course, the above limiting process is complex, but it should be pointed out that Eq. (25) is the combined form for the point z_0' being on the upper and lower surface of a crack. Therefore, in applying (25), the upper and lower surfaces of a crack need not be considered separately.

For the orthotropic cases, there is further relation [21,27]

$$U_{ij}(z_0,z) = U_{ji}(z_0,z). \tag{26}$$

Noticing Eqs. (6), (9), (10) and (11), we have

$$c_{lmik}U_{ij,k}(z_0,z) = c_{lmik}U_{ji,k}(z_0,z) = -D_{jlm}(z_0,z). \tag{27}$$

So, Eq. (25) becomes

$$\begin{aligned}
&n_m(z_0)\int_S D_{jlm}(z_0,z)t_j(z)\mathrm{d}s(z) - n_m(z_0)\int_S W_{jlm}(z_0,z)\frac{\partial u_j(z)}{\partial s(z)}\mathrm{d}s(z) + n_m(z_0)\int_\Gamma D_{jlm}(z_0,z)\sum t_j(z)\mathrm{d}s(z)\\
&-n_m(z_0)\int_\Gamma W_{jlm}(z_0,z)\frac{\partial \Delta u_j(z)}{\partial s(z)}\mathrm{d}s(z) = \begin{cases}\frac{1}{2}t_l(z_0) & z_0\in s\\ \frac{1}{2}\left(t_l(z_0^+)-t_l(z_0^-)\right) & z_0\in \Gamma\end{cases}.
\end{aligned} \tag{28}$$

Because integration by parts is skillfully used, the new traction boundary integral equations (25) and (28) do not involve hypersingular terms, and it will be very helpful for the numerical computation. On the other hand, the integration by parts produces the new variables $\partial u_i/\partial s$ and $\partial \Delta u_i/\partial s$ with the physical meaning: the displacement densities and dislocation densities. We will give the relations between the stress intensity factors and the dislocation densities to evaluate SIF in Section 6. Moreover, all the crack boundary conditions (both upper and lower ones) have been incorporated into (28), thus, there is no need to discretize the upper and lower crack surfaces separately when boundary element method is applied. Compared with the dual BEM [15,22], no displacement boundary integral equation is required in applying (28) to crack problems, and (28) can be directly used for the general boundary and crack surface.

Previously, Chau and Wang [12] and Wang [11] have make use of integration by parts to 2-D and 3-D isotropic crack problems and induced the boundary integral equations similar to (28). In their works [11,12], they also obtained some significative analytical solutions. But (28) is difficult for the theoretical analysis, we will establish the BEM numerical frame based on (28) in the next section.

4. Numerical implementation of boundary element

The numerical treatment of (25) or (28) requires that all boundaries be discretized into a series of segments. As shown in Fig. 1, the boundary S and the crack surface Γ can be replaced by an assembly of linear elements [13]. The variable x_i ($i = 1,2$) on each element can be expressed as

$$x_i = N_1(\xi)x_i^{(1)} + N_2(\xi)x_i^{(2)}, \quad (|\xi| \leqslant 1), \tag{29}$$

where the shape functions are defined as

$$N_1(\xi) = \frac{1}{2}(1-\xi), \quad N_2(\xi) = \frac{1}{2}(1+\xi), \tag{30}$$

with $(x_1^{(1)}, x_2^{(1)})$ and $(x_1^{(2)}, x_2^{(2)})$ are the coordinates of the initial and end node of the element respectively.

When an element does not contain any crack tip, the following interpolation functions are used

$$\begin{aligned} &\frac{\partial u_i}{\partial s} = N_1(\xi)\frac{\partial u_i^{(1)}}{\partial s} + N_2(\xi)\frac{\partial u_i^{(2)}}{\partial s} \quad \text{for the general boundary,} \\ &t_i = N_1(\xi)t_i^{(1)} + N_2(\xi)t_i^{(2)} \end{aligned} \tag{31}$$

or

$$\begin{aligned} &\frac{\partial \Delta u_i}{\partial s} = N_1(\xi)\frac{\partial \Delta u_i^{(1)}}{\partial s} + N_2(\xi)\frac{\partial \Delta u_i^{(2)}}{\partial s} \quad \text{for the crack surface,} \\ &\sum t_i = N_1(\xi)\sum t_i^{(1)} + N_2(\xi)\sum t_i^{(2)} \end{aligned} \tag{32}$$

where $\partial u_i^{(k)}/\partial s, \partial \Delta u_i^{(k)}/\partial s, t_i^{(k)}$ and $\sum t_i^{(k)}$ $(k = 1, 2)$ denote the nodal values of the functions.

Otherwise, if the local node 1 ($\xi = -1$) of an element is at a crack tip, the function $\partial \Delta u_i/\partial s$ with the singular behavior at a crack tip can be approximated by

$$\frac{\partial \Delta u_i}{\partial s} = \frac{\partial \Delta u_i^{*(1)}}{\partial s} \Bigg/ \sqrt{N_2(\xi)} + N_2(\xi)\left(\frac{\partial \Delta u_i^{(2)}}{\partial s} - \frac{\partial \Delta u_i^{*(1)}}{\partial s}\right). \tag{33}$$

Similarly, in the case of the element node 2 ($\xi = 1$) being a crack tip, $\partial \Delta u_i/\partial s$ can be represented by

$$\frac{\partial \Delta u_i}{\partial s} = \frac{\partial \Delta u_i^{*(2)}}{\partial s} \Bigg/ \sqrt{N_1(\xi)} + N_1(\xi)\left(\frac{\partial \Delta u_i^{(1)}}{\partial s} - \frac{\partial \Delta u_i^{*(2)}}{\partial s}\right). \tag{34}$$

On the crack tip elements, the traction sum can be interpolated with the second formula of (32).

Discretizing the boundary integral equations (25) or (28) on all boundaries and considering for it at the midpoint $z_0(x_{01}, x_{02})$ of each of the elements in turn, we obtain a system of linear algebraic equations. In addition, solving the system requires the following condition for single-valuedness of displacement

$$\int_\Gamma \frac{\partial \Delta u_i}{\partial s}\,\mathrm{d}s = 0. \tag{35}$$

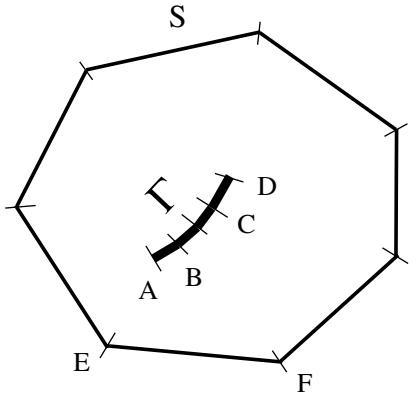

Fig. 1. Discretized elements on the boundary and crack surface.

5. Evaluation of singular integrals

In the numerical performance of BEM, the treatment of the singular integrals has a large effect on the accuracy of the numerical results. Because our method bypasses the hypersingular integral, all singular integrals can be analytically computed. We will discuss the evaluation of singular integrals in this section.

As mentioned in the previous, the boundary integral in (28) can be modeled by the sum of element integrals, that is, $\int_{S+\Gamma}(\cdots)\mathrm{d}s(z) = \sum \int_{L_e}(\cdots)\mathrm{d}s(z)$, in which the ordinary element integrals can be evaluated by the standard Gauss–Legendre integration formula. However, when the source point z_0 is on the L_e, we have to handle the singular integrals in the form (the kernel $W_{ijk}(z_0,z)$ is the combination of $D_{lmn}(z_0,z)$)

$$\int_{L_e} D_{lmn}(z_0,z) f(z)\,\mathrm{d}s(z),$$

where $f(z)$ corresponds to $t_i(z)$, $\sum t_i(z)$, $\partial u_i(z)/\partial s$ or $\partial \Delta u_i(z)/\partial s$.

As an example, the evaluation of $\int_{L_e} D_{111} f(z)\,\mathrm{d}s(z)$ is given here. Defining the coordinates of the point $P(x_0,y_0)$ as $x_0 = x_1N_1(\xi_0) + x_2N_2(\xi_0)$ and $y_0 = y_1N_1(\xi_0) + y_2N_2(\xi_0)$ ($|\xi_0| < 1$), and noticing (11), one can obtain

$$\int_{L_e} D_{111}(z_0,z) f(z)\,\mathrm{d}s(z) = -2|L_e| Re\left[\sum_{j=1}^{2} L_{1j}\mu_j A_{1j} \frac{1}{(x_2-x_1)-\mu_j(y_2-y_1)}\right] \int_{-1}^{1} \frac{f(Q(\xi))}{\xi-\xi_0}\,\mathrm{d}\xi, \tag{36}$$

where $|L_e|$ denotes the length of the element L_e.

Now, the problem becomes into the evaluation of the integral $\int_{-1}^{1} \frac{f(Q(\xi))}{\xi-\xi_0}\,\mathrm{d}\xi$. Considering (31)–(34), the exact solutions of the integral $\int_{-1}^{1} \frac{f(Q(\xi))}{\xi-\xi_0}\,\mathrm{d}\xi$ are listed as follows:

$$\int_{-1}^{1} \frac{f(Q(\xi))}{\xi-\xi_0}\,\mathrm{d}\xi = f(Q(\xi_0)) \ln\left|\frac{1-\xi_0}{1+\xi_0}\right| + (f_2 - f_1), \quad \text{for general elements;}$$

$$\int_{-1}^{1} \frac{f(Q(\xi))}{\xi-\xi_0}\,\mathrm{d}\xi = \frac{f_1}{\sqrt{N_2(\xi_0)}} \ln\left|\frac{1-\sqrt{N_2(\xi_0)}}{1+\sqrt{N_2(\xi_0)}}\right| + (f_2-f_1)N_2(\xi_0)\ln\left|\frac{1-\xi_0}{1+\xi_0}\right| + (f_2-f_1),$$

for initial crack tip elements and $f(Q(\xi))$ corresponding to $\partial \Delta u_i/\partial s$;

$$\int_{-1}^{1} \frac{f(Q(\xi))}{\xi-\xi_0}\,\mathrm{d}\xi = -\frac{f_2}{\sqrt{N_1(\xi_0)}} \ln\left|\frac{1-\sqrt{N_1(\xi_0)}}{1+\sqrt{N_1(\xi_0)}}\right| + (f_1-f_2)N_1(\xi_0)\ln\left|\frac{1-\xi_0}{1+\xi_0}\right| + (f_2-f_1),$$

for end crack tip elements and $f(Q(\xi))$ corresponding to $\partial \Delta u_i/\partial s$. (37)

If z_0 is taken as the midpoint of a singular element, as what we proposed in the previous section, ξ_0 in (37) is zero.

In addition, when the collocation point z_0 is on the general element and the integral is performed on the crack tip element, noticing (33) and (34), the singular integral $\int_{-1}^{1} \frac{1}{\sqrt{1-\xi}}\,\mathrm{d}\xi$ or $\int_{-1}^{1} \frac{1}{\sqrt{1+\xi}}\,\mathrm{d}\xi$ appears, and they are easily calculated as the generalized integral.

An attractive feature of the present formulation is that since all singular integrands are evaluated exactly, our proposed numerical scheme is free from numerical problems arising from integrating singular integrals.

6. Stress intensity factors

For the mode I fracture problem of an anisotropic body, the displacements (Fig. 2) in a small region surrounding the crack tip are [2,25]

$$\begin{aligned} u_1^{\mathrm{I}} &= K_{\mathrm{I}}\sqrt{\frac{2r}{\pi}}Re\left[\frac{1}{\mu_1-\mu_2}\left(\mu_1 P_{12}\sqrt{\cos\theta+\mu_2\sin\theta}-\mu_2 P_{11}\sqrt{\cos\theta+\mu_1\sin\theta}\right)\right], \\ u_2^{\mathrm{I}} &= K_{\mathrm{I}}\sqrt{\frac{2r}{\pi}}Re\left[\frac{1}{\mu_1-\mu_2}\left(\mu_1 P_{22}\sqrt{\cos\theta+\mu_2\sin\theta}-\mu_2 P_{21}\sqrt{\cos\theta+\mu_1\sin\theta}\right)\right], \end{aligned} \tag{38}$$

where K_{I} is the mode I stress intensity factor.

We can differentiate u_i^{I} with respect to x_1 and let $\theta = 180^\circ$ to give

$$\begin{aligned} \frac{\partial\Delta u_1}{\partial s} &= K_{\mathrm{I}}\sqrt{\frac{2}{\pi r}}\mathrm{Im}\left(\frac{\mu_1 P_{12}-\mu_2 P_{11}}{\mu_1-\mu_2}\right), \\ \frac{\partial\Delta u_2}{\partial s} &= K_{\mathrm{I}}\sqrt{\frac{2}{\pi r}}\mathrm{Im}\left(\frac{\mu_1 P_{22}-\mu_2 P_{21}}{\mu_1-\mu_2}\right). \end{aligned} \tag{39}$$

For mode II, the similar relations are

$$\begin{aligned} u_1^{\mathrm{II}} &= K_{\mathrm{II}}\sqrt{\frac{2r}{\pi}}Re\left[\frac{1}{\mu_1-\mu_2}\left(P_{12}\sqrt{\cos\theta+\mu_2\sin\theta}-P_{11}\sqrt{\cos\theta+\mu_1\sin\theta}\right)\right], \\ u_2^{\mathrm{II}} &= K_{\mathrm{II}}\sqrt{\frac{2r}{\pi}}Re\left[\frac{1}{\mu_1-\mu_2}\left(P_{22}\sqrt{\cos\theta+\mu_2\sin\theta}-P_{21}\sqrt{\cos\theta+\mu_1\sin\theta}\right)\right], \end{aligned} \tag{40}$$

and

$$\begin{aligned} \frac{\partial\Delta u_1}{\partial s} &= K_{\mathrm{II}}\sqrt{\frac{2}{\pi r}}\mathrm{Im}\left(\frac{P_{12}-P_{11}}{\mu_1-\mu_2}\right), \\ \frac{\partial\Delta u_2}{\partial s} &= K_{\mathrm{II}}\sqrt{\frac{2}{\pi r}}\mathrm{Im}\left(\frac{P_{22}-P_{21}}{\mu_1-\mu_2}\right), \end{aligned} \tag{41}$$

where K_{II} is the mode II stress intensity factor.

So, for mixed mode problems we have

$$\begin{aligned} \frac{\partial\Delta u_1}{\partial s} &= K_{\mathrm{I}}\sqrt{\frac{2}{\pi r}}\mathrm{Im}\left(\frac{\mu_1 P_{12}-\mu_2 P_{11}}{\mu_1-\mu_2}\right)+K_{\mathrm{II}}\sqrt{\frac{2}{\pi r}}\mathrm{Im}\left(\frac{P_{12}-P_{11}}{\mu_1-\mu_2}\right), \\ \frac{\partial\Delta u_2}{\partial s} &= K_{\mathrm{I}}\sqrt{\frac{2}{\pi r}}\mathrm{Im}\left(\frac{\mu_1 P_{22}-\mu_2 P_{21}}{\mu_1-\mu_2}\right)+K_{\mathrm{II}}\sqrt{\frac{2}{\pi r}}\mathrm{Im}\left(\frac{P_{22}-P_{21}}{\mu_1-\mu_2}\right). \end{aligned} \tag{42}$$

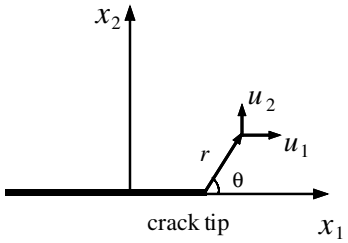

Fig. 2. Displacement field surrounding the crack tip.

Considering Eqs. (33) and (34), the above equation can be written as

$$\begin{aligned} K_{\mathrm{I}}\mathrm{Im}\left(\frac{\mu_1 P_{12}-\mu_2 P_{11}}{\mu_1-\mu_2}\right)+K_{\mathrm{II}}\mathrm{Im}\left(\frac{P_{12}-P_{11}}{\mu_1-\mu_2}\right)&=\lim_{r\to 0}\frac{\partial\Delta u_1}{\partial s}\sqrt{\frac{\pi r}{2}}\sim\frac{\partial\Delta u_1^{*(1)}}{\partial s}\quad\text{or}\quad\frac{\partial\Delta u_1^{*(2)}}{\partial s},\\ K_{\mathrm{I}}\mathrm{Im}\left(\frac{\mu_1 P_{22}-\mu_2 P_{21}}{\mu_1-\mu_2}\right)+K_{\mathrm{II}}\mathrm{Im}\left(\frac{P_{22}-P_{21}}{\mu_1-\mu_2}\right)&=\lim_{r\to 0}\frac{\partial\Delta u_2}{\partial s}\sqrt{\frac{\pi r}{2}}\sim\frac{\partial\Delta u_2^{*(1)}}{\partial s}\quad\text{or}\quad\frac{\partial\Delta u_2^{*(2)}}{\partial s}. \end{aligned} \tag{43}$$

Eqs. (42) and (43) indicate that the dislocation density $\partial\Delta u_i/\partial s$ near the crack tip shows the singularity in the order of $1/\sqrt{r}$ and K_{I}, K_{II} are in linear relation to the unknowns $\partial\Delta u_i^{*(1)}/\partial s$ or $\partial\Delta u_i^{*(2)}/\partial s$ in Eq. (33) or (34). So, the stress intensity factor can be calculated after $\partial\Delta u_i^{*(1)}/\partial s$ or $\partial\Delta u_i^{*(2)}/\partial s$ are obtained.

7. Numerical examples

The above boundary element method was written into the program using the standard FORTRAN 90, and four examples were selected to illustrate the accuracy and validity of the present method. All examples assume plane stress.

7.1. Central crack in a rectangular plate

The first example is an orthotropic rectangular plate containing a central crack of length $2a$ (see Fig. 3 and let $\alpha = 0$). The axes of elastic symmetry of orthotropic plate coincide with the axes x_1 and x_2. The plate is subjected to uniform stress of magnitude σ along the x_2-direction, and the problem is pure mode I. Only four elastic constants are independent [24,25]

$$s_{11}=1/E_1,\quad s_{22}=1/E_2,\quad s_{66}=1/\mu_{12},\quad s_{12}=-\nu_{12}/E_1=-\nu_{21}/E_2, \tag{44}$$

E_1, E_2 are the Young's moduli, μ_{12} is the shear moduli and ν_{12}, ν_{21} are the Poisson's ratios. The introduced variables β_1 and β_2 are related to the elastic constants in the following way [28]

$$\beta_1\beta_2=(E_1/E_2)^{1/2},\quad \beta_1+\beta_2=\sqrt{2}\left[(E_1/E_2)^{1/2}+E_1/2\mu_{12}-\nu_{12}\right]^{1/2}. \tag{45}$$

In the calculation, the variable β_1 is taken as 1.0 and the plate dimensions are fixed as $h = b$. The normalized mode I stress intensity factor $Y_{\mathrm{I}} = K_{\mathrm{I}}/\sigma\sqrt{\pi a}$ for different values of a/b and β_2^2 are presented in Table 1, together with those obtained by Bowie and Freese [17], and the results are also plotted in Fig. 4.

7.2. Central slant crack in a rectangular plate

The second example is a central slant crack in a rectangular plate under uniform tension in x_2-direction (Fig. 3). The crack is inclined at 45° to the x_1-direction ($\alpha = 45°$). The material is orthotropic with $E_1 = 48.26$ GPa, $E_2 = 17.24$ GPa, $G_{12} = 6.89$ GPa and $\nu_{12} = 0.29$ [2,19] and the direction of material fibers was rotated from $\beta = 0°$ to $\beta = 180°$. The plate dimensions are: $h/b = 2.0$ and $a/b = 0.2$. The numerical results for different angle β are presented in Table 2. The problem was also computed by Sollero and Aliabadi [2] and Pan and Amadei [22], here, only the results by Gandhi [16] are listed and compared with ours.

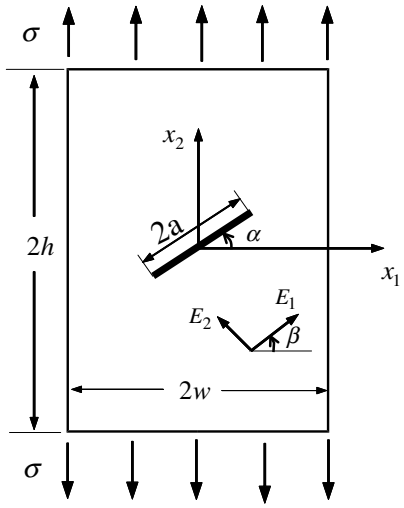

Fig. 3. Central crack in a rectangular anisotropic plate.

Table 1
The normalized mode I stress intensity factor $Y_I = K_I/\sigma\sqrt{\pi a}$ for different values of a/b and β_2^2

a/b	$\beta_2^2 = 0.1$		$\beta_2^2 = 0.5$		$\beta_2^2 = 1.5$		$\beta_2^2 = 2.5$	
	Present	Bowie and Freese [17]	Present	Bowie and Freese [17]	Present	Bowie and Freese [17]	Present	Bowie and Freese [17]
0.1	1.026	1.04	1.011	1.02	1.008	1.01	1.006	1.01
0.2	1.151	1.16	1.060	1.08	1.028	1.05	1.034	1.04
0.3	1.334	1.34	1.155	1.17	1.084	1.10	1.082	1.08
0.4	1.570	1.57	1.287	1.30	1.164	1.18	1.149	1.15
0.5	1.868	1.85	1.452	1.46	1.271	1.28	1.241	1.24
0.6	2.257	2.20	1.644	1.64	1.402	1.41	1.365	1.36
0.7	2.709	2.63	1.883	1.86	1.595	1.59	1.555	1.53

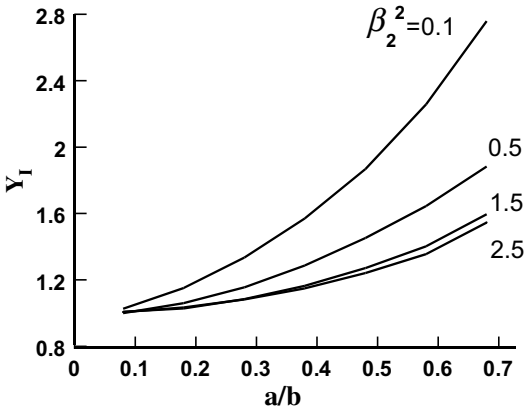

Fig. 4. Variation of the normalized mode I stress intensity factor $Y_I = K_I/\sigma\sqrt{\pi a}$ with a/b for different values of β_2^2.

Table 2
Normalized stress intensity factors for a central inclined crack in an orthotropic rectangular plate

α	$K_I/(\sigma\sqrt{\pi a})$		$K_{II}/(\sigma\sqrt{\pi a})$	
	Present	Gandhi [16]	Present	Gandhi [16]
0	0.5219	0.522	0.5060	0.507
45	0.5145	0.515	0.5033	0.505
90	0.5121	0.513	0.5075	0.509
105	0.5153	0.517	0.5092	0.510
120	0.5233	0.524	0.5104	0.512
135	0.5312	0.532	0.5100	0.511
180	0.5219	0.522	0.5060	0.507

7.3. Kinked crack in the infinite orthotropic media

In this example, we consider a kinked crack in the infinite orthotropic medium under a uniform far-field stress in the x_2-direction (Fig. 5). Two principle directions of the material are along the axes x_1 and x_2, and the same anisotropic constants with those in 7.2 are used. θ denotes the angle between the main crack and the branched part. First, the ratio of the branched part to the horizontal part is taken as $b/a = 0.2$, and the normalized stress intensity factors $Y_I = K_I/\sigma\sqrt{\pi a}$ and $Y_{II} = K_{II}/\sigma\sqrt{\pi a}$ at points A and B for different values of θ are calculated and given in Table 3. When the angle θ is equal to 0, the problem induced to the case for a single straight crack.

The stress intensity factors for $b/a = 0.1$ and 0.05 are also calculated and all results are presented in Figs. 6–9. It can be seen that Y_I and Y_{II} are symmetric and anti-symmetric solutions with respect to θ respectively and the variations of Y_I and Y_{II} are similar to those of isotropic medium [13].

In the neighbourhood of the kinked crack vertex, the stress is singular like r^{-s} with $s < \frac{1}{2}$, r is the radius distance to the vertex [29]. This has not always been taken into account. Pan and Amadei [22], Melin [30] and Vitek [31], for example, did not consider this singularity in their analyses. Karihaloo et al. [32] pointed out that the singularity near the vertex is weaker than at the crack tip, but their analysis proceeds with a singularity $r^{-1/2}$ at the vertex. In our calculation, the singularity at the vertex is not considered. Two hundred elements were used for the main crack, and the branched part was modeled using 40, 20 and 10 elements for $b/a = 0.2$, 0.1 and 0.05 respectively.

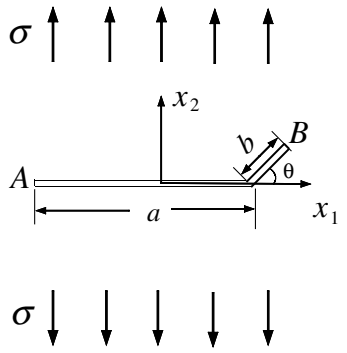

Fig. 5. A kinked crack in the infinite orthotropic medium.

Table 3
Normalized stress intensity factors for a kinked crack ($b/a = 0.2$) in an infinite anisotropic medium

θ (°)	$K_{\mathrm{I}}^{A}/\sigma\sqrt{\pi a}$	$K_{\mathrm{II}}^{A}/\sigma\sqrt{\pi a}$	$K_{\mathrm{I}}^{B}/\sigma\sqrt{\pi a}$	$K_{\mathrm{II}}^{B}/\sigma\sqrt{\pi a}$
0	0.7717	0.0	0.7717	0.0
15	0.7683	−0.0161	0.7303	0.1753
30	0.7620	−0.0248	0.6124	0.3344
45	0.7491	−0.0257	0.4384	0.4427
60	0.7376	−0.0208	0.2402	0.4780
75	0.7271	−0.0122	0.0521	0.4399

The exact results for $\theta = 0 : K_{\mathrm{I}}^{A}/\sigma\sqrt{\pi a} = K_{\mathrm{I}}^{B}/\sigma\sqrt{\pi a} = 0.7746$.

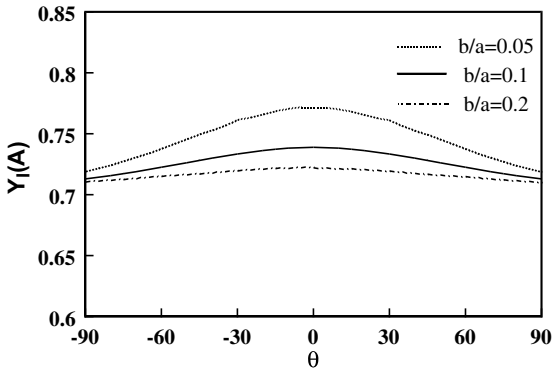

Fig. 6. Variation of the normalized mode I stress intensity factor $Y_{\mathrm{I}}(A) = K_{\mathrm{I}}^{A}/\sigma\sqrt{\pi a}$ with θ for $b/a = 0.05$, 0.1 and 0.2.

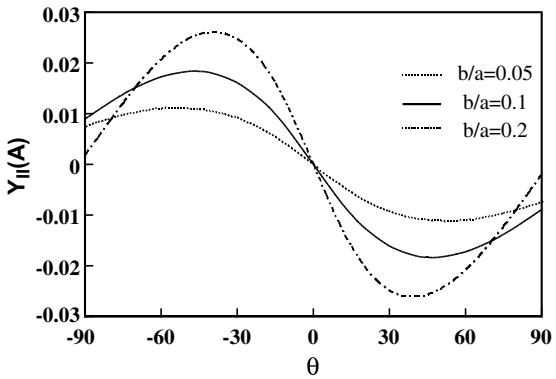

Fig. 7. Variation of the normalized mode II stress intensity factor $Y_{\mathrm{II}}(A) = K_{\mathrm{II}}^{A}/\sigma\sqrt{\pi a}$ with θ for $b/a = 0.05$, 0.1 and 0.2.

7.4. Circular-arc crack in the infinite orthotropic media

To demonstrate the validity of our method for the curved crack, the circular-arc crack in the infinite orthotropic media is considered (Fig. 10). The crack region is under uniform tension σ in two perpendicular

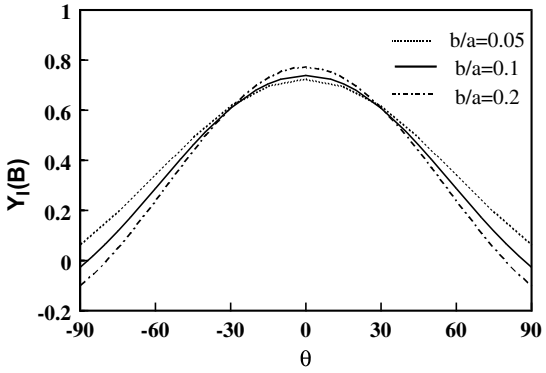

Fig. 8. Variation of the normalized mode I stress intensity factor $Y_I(B) = K_I^B/\sigma\sqrt{\pi a}$ with θ for $b/a = 0.05$, 0.1 and 0.2.

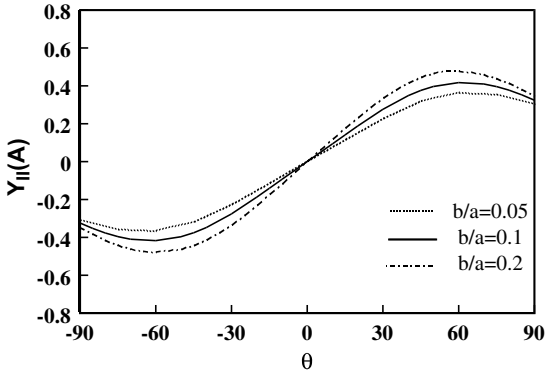

Fig. 9. Variation of the normalized mode II stress intensity factor $Y_{II}(B) = K_{II}^B/\sigma\sqrt{\pi a}$ with θ for $b/a = 0.05$, 0.1 and 0.2.

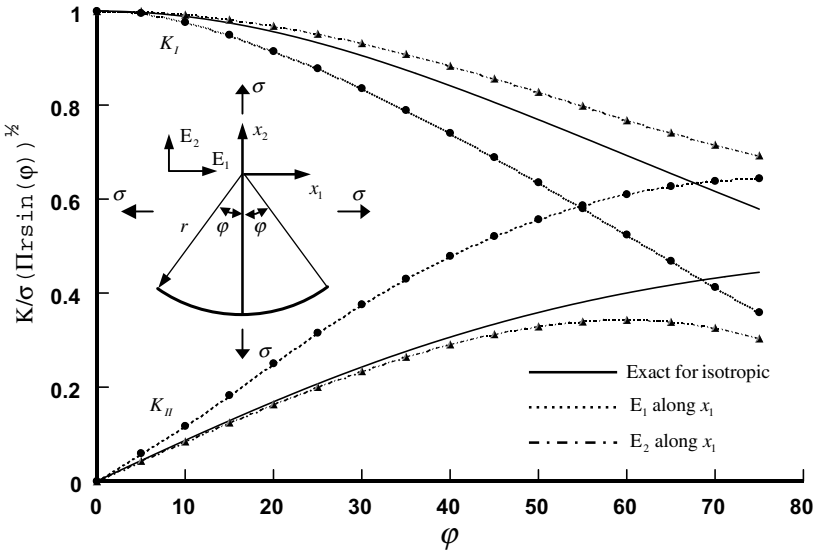

Fig. 10. The normalized mode I and II stress intensity factors for a circular-arc crack under equi-biaxial tension in an unbounded anisotropic media.

directions. No analytical solution has been found for this problem, Gao and Chiu [33] studied this problem using perturbation analysis method and proposed that the stress intensity factors K_I, K_{II} maybe be close to the those of isotropic case when the semi-angle is smaller.

In our calculation, the elastic constants $E_1 = 138.9$ GPa, $E_2 = 8.96$ GPa, $G_{12} = 7.1$ GPa and $v_{12} = 0.3$ [34] are used, two cases for the stiffer material axis E_1 and weaker material axis E_2 along the direction x_1 are computed, the normalized stress intensity factors $Y_{I,II} = K_{I,II}/\sigma(\pi r \sin(\varphi))^{1/2}$, as the function of the semi-angle φ, are plotted in Fig. 10 with the exact solutions for isotropic case [35]. Recently, Garcia et al. [34] also calculated this problem, but they only gave the results for the case that weaker material axis E_2 is along the direction x_1. Careful comparison showed that our results are very close to those by Garcia et al. [34], and the largest difference about Y_{II} is 0.01 ($\varphi = 75°$). It can also be seen that the results are close to those of isotropic case only when the weaker material axis is along x_1 and the prediction of Gao and Chiu [33] seems to be unsuccessful.

8. Conclusions

A simple and efficient BEM formulation for cracked 2-D anisotropic media is proposed, and it involves only singularity in the order of $1/r$. The boundary conditions on the crack surface are incorporated into and the upper and lower surfaces do not need be considering separately. Not like the dual BEM, the displacement boundary integral equation is not required while the BEM is performed. It can directly be used to the 2-D anisotropic problems with arbitrary cracks, boundaries. The relations between the stress intensity factors and the dislocation density $\partial \Delta u_i/\partial s$ near the crack tip are given. The BEM based on the new boundary integral equations is established, and singular interpolation functions are introduced on the crack tip elements.

The paper presents a new technique for crack problems and the method in this paper can be universally used to handle other linear elastic fracture mechanics problems, for examples cracked isotropic or anisotropic bodies under anti-plane shear [36,37].

References

[1] Snyder MD, Cruse TA. Boundary-integral equation analysis of cracked anisotropic plates. Int J Fract 1975;11:315–28.
[2] Sollero P, Aliabadi MH. Fracture mechanics analysis of anisotropic plates by the boundary element method. Int J Fract 1993;64:269–84.
[3] Wang YH, Cheung YK, Woo CW. Anti-plane shear problem for an edge crack in a finite orthotropic plate. Engng Fract Mech 1992;42:971–6.
[4] Crouch SL. Solution of plane elasticity problems by the displacement discontinuity method. Int J Numer Meth Engng 1976;10:301–43.
[5] Hong HK, Chen JT. Derivations of integral-equations of elasticity. J Engng Mech-ASCE 1988;114(6):1028–44.
[6] Gray LJ. Boundary element method for regions with thin integral cavities. Engng Anal Bound Elem 1989;6(4):180–4.
[7] Portela A, Aliabadi MH, Rooke DP. The dual boundary element method: effective implementation for crack problems. Int J Numer Meth Engng 1992;33:1269–87.
[8] Bui HD. An integral equations methods for solving the problem of a plane crack of arbitrary shape. J Mech Phys Solids 1977;25:29–39.
[9] Weaver J. Three-dimensional crack analysis. Int J Solids Struct 1977;13:321–30.
[10] Wang YB. A boundary integral equation method for The Griffith crack problem under asymmetric loading. J Lanzhou Univ (Nat Sci) 1990;26:35–9 [in Chinese].
[11] Wang YB. A new boundary integral equation method of three-dimensional crack analysis. Int J Fract 1993;63:317–28.
[12] Chau KT, Wang YB. A new boundary integral formulation for plane elastic bodies containing cracks and holes. Int J Solids Struct 1999;36:2041–74.
[13] Wang YB, Chau KT. A new boundary element for plane elastic problems involving cracks and holes. Int J Fract 1997;87:1–20.

[14] Richardson JD, Cruse TA. Weakly singular stress-BEM for 2D elastostatics. Int J Numer Meth Engng 1999;45(1):13–35.
[15] Li S, Mear ME, Xiao L. Symmetric weak-form integral equation method for three-dimensional fracture analysis. Comput Meth Appl Mech Engng 1998;151(3–4):435–59.
[16] Gandhi KR. Analysis of an inclined crack centrally placed in an orthotropic rectangular plate. J Strain Anal 1972;7:157–62.
[17] Bowie OL, Freese CE. Central crack in plane orthotropic rectangular sheet. Int J Fract 1972;8:49–58.
[18] Chu SJ, Hong CS. The application of J'_k integral to mixed mode crack problems for anisotropic composite laminates. Engng Fract Mech 1990;35:1093–103.
[19] Yum YJ, Hong CS. Stress intensity factors in finite orthotropic plates with a crack under mixed mode deformation. Engng Fract Mech 1991;47:53–6.
[20] Kamel M, Liaw BM. Boundary element formulation with special kernels for an anisotropic plate containing an elliptical hole or crack. Engng Fract Mech 1991;39:695–711.
[21] Doblare M, Espiga F, Alcantud M. Study of crack propagation on orthotropic materials by using boundary element method. Engng Fract Mech 1990;37:953–67.
[22] Pan E, Amadei B. Fracture mechanics analysis of cracked 2-D anisotropic media with a new formulation of the boundary element method. Int J Fract 1996;77:161–74.
[23] Gray LJ, Paulino GH. Symmetric Galerkin boundary integral fracture analysis for plane orthotropic elasticity. Comput Mech 1997;20(1–2):26–33.
[24] Vinson JR, Sierakowski. The behavior structures composed of composite materials. Dordrecht: Martinus Nijhoff; 1987 [chapters 1–3].
[25] Sih GC, Chen EP. Cracks in materials possessing homogeneous anisotropic. In: Sih GC, editor. Mechanics of fracture, vol. 6. The Hague: Martinus Nijhoff; 1981.
[26] Rizzo FJ, Shippy DJ. A method for stress determination in plane anisotropic elastic bodies. J Compos Mater 1970;4:36–61.
[27] Brebbia CA, Telles JCF, Wrobel LC. Boundary element techniques. Berlin: Springer-Verlag; 1984.
[28] Sih GC. Handbook of stress intensity factors. Bethlehem Pennsylvania: Lehigh University; 1973.
[29] Bogy DB. Two edge-bonded elastic wedges of different materials and wedge angles under surface tractions. J Appl Mech 1971;38:377–86.
[30] Melin S. On singular integral equations for kinked cracks. Int J Fract 1986;30:57–65.
[31] Vitek V. Plane strain stress intensity factors for branched cracks. Int J Fract 1977;13:481–501.
[32] Karihaloo BL, Keer LM, Nemat-Nasser S. Crack kinking under nonsymmetric loading. Engng Fract Mech 1980;13:879–88.
[33] Gao HJ, Chiu CH. Slightly curved or kinked cracks in anisotropic elastic solids. Int J Solids Struct 1992;29(8):947–72.
[34] Garcia F, Saez A, Dominguez J. Traction boundary elements for cracks in anisotropic solids. Engng Anal Bound Elem 2004;28(6):667–76.
[35] Muskhelishivili NI. Some basic problems of the mathematical theory of elasticity. Leiden: Noordhoff; 1953.
[36] Sun YZ, Wang YB. Boundary element method for anti-plane crack problems. J Lanzhou Univ (Nat Sci) 2001;37(4):25–31 [in Chinese].
[37] Sun YZ, Yang SS, Wang YB. A new formulation of boundary element method for cracked anisotropic bodies under anti-plane shear. Comput Meth Appl Mech Engng 2003;192(22–24):2633–48.